

EvRWKV: A RWKV Framework for Effective Event-guided Low-Light Image Enhancement

WenJie Cai*, Qingguo Meng*✉, Zhenyu Wang, Xingbo Dong, Zhe Jin

Abstract—Capturing high-quality visual content under low-light conditions remains a challenging problem due to severe noise, motion blur, and underexposure, which degrade the performance of downstream applications. Traditional frame-based low-light enhancement methods often amplify noise or fail to preserve structural details, especially in real-world scenarios. Event cameras, offering high dynamic range and microsecond temporal resolution by asynchronously capturing brightness changes, emerge as promising alternatives for low-light imaging. However, existing event-image fusion methods suffer from simplistic fusion strategies and inadequate handling of spatial-temporal misalignment and noise. To address these challenges, we propose EvRWKV, a novel framework that enables continuous cross-modal interaction through dual-domain processing. Our approach incorporates a Cross-RWKV module, leveraging the Receptance Weighted Key Value (RWKV) architecture for fine-grained temporal and cross-modal fusion, and an Event Image Spectral Fusion Enhancer (EISFE) module, which jointly performs adaptive frequency-domain noise suppression and spatial-domain deformable convolution alignment. Extensive qualitative and quantitative evaluations on real-world low-light datasets (SDE, SDS, RELED) demonstrate that EvRWKV achieves state-of-the-art performance, effectively enhancing image quality by suppressing noise, restoring structural details, and improving visual clarity in challenging low-light conditions.

Index Terms—Low-light image enhancement, event cameras, cross-modal fusion, RWKV, frequency-domain filtering, noise suppression, spatiotemporal alignment.

I. INTRODUCTION

CAPTURING high-quality visual content under low-light conditions remains a critical yet challenging task in computer vision [25]. Images and videos acquired in such environments often suffer from severe noise, motion blur, and underexposure [25], which degrade downstream applications such as autonomous driving and surveillance. Traditional frame-based low-light image enhancement methods [22, 43, 8, 46] have made progress, but often struggle to effectively address the inherent complexities of real-world low-light scenarios. Many methods [51, 3, 45, 30, 25] can amplify existing noise while attempting to brighten the image, leading to visually unappealing results. Furthermore, approaches relying on synthetic data for training often fail to generalize well to the diverse and unpredictable nature of real-world low-light scenes.

Manuscript created October, 2020; This work was developed by the IEEE Publication Technology Department. This work is distributed under the L^AT_EX Project Public License (LPPL) (<http://www.latex-project.org/>) version 1.3. A copy of the LPPL, version 1.3, is included in the base L^AT_EX documentation of all distributions of L^AT_EX released 2003/12/01 or later. The opinions expressed here are entirely that of the author. No warranty is expressed or implied. User assumes all risk.

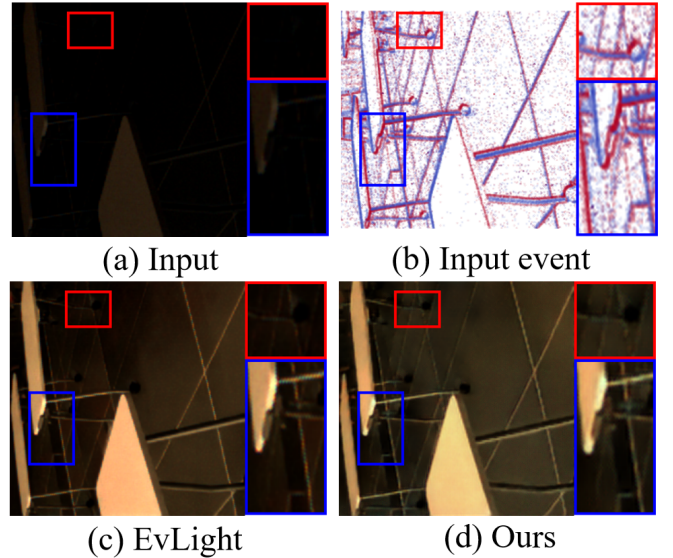


Fig. 1. A challenging example from our dataset containing an extremely low-light image (a) and sparse events (b). Compared with the result from the SOTA event-guided method EvLight (c), our EvRWKV (d) not only recovers the wheel details in the dark areas (e.g., the wheel) but also preserves edge details (e.g., the white line on the floor).

Event cameras, using bio-inspired sensors [29], are widely used in the field of computer vision due to their high dynamic range and microsecond level time resolution [40, 55], such as image restoration [16], video super-resolution [34], optical flow [35], deblurring [17, 18], etc., and have also become a promising alternative to low-light imaging scenes. By asynchronously capturing per-pixel brightness changes, events excel at preserving structural details even in extreme darkness and are less susceptible to motion blur. This makes them particularly attractive for low-light enhancement, where traditional cameras struggle due to signal-to-noise ratio limitations and motion artifacts. However, exploiting event cameras for low-light enhancement is not straightforward. Existing methods [41, 39] that rely solely on event cameras often face limitations due to the sparse nature of the event data, which can lead to poor spatial resolution and difficulty in handling noise under extreme low light conditions. Furthermore, fusion techniques combining events and images often use simplistic approaches [16, 42, 33, 28], which fail to effectively capture the complex spatial-temporal interactions between them. As a result, these methods do not fully leverage the complementary strengths of event and image data, limiting their performance in low-light enhancement tasks.

A major limitation of current event and image fusion

techniques lies in their simplistic handling of these distinct data streams. Many existing methods [16, 42, 33] process events and images through separate pathways and then perform rudimentary fusion, typically by concatenating or adding features from both modalities. This decoupled approach fails to fully exploit the rich, cross-modal relationships inherent in simultaneously captured event and image data. In particular, fine-grained spatial-temporal interactions between the high-frequency dynamics of events and the textural information in images are often overlooked, leading to suboptimal fusion. Furthermore, both modalities are vulnerable to noise, including event noise in extreme darkness [9] and image sensor noise [25], and these basic fusion strategies may amplify such noise interference, resulting in further deterioration of enhancement quality. A fundamental challenge arises from the structural mismatch between the event data, which is temporally continuous but spatially sparse [29], and the images, which offer dense spatial sampling but with limited temporal resolution [25]. This discrepancy hinders effective integration of the motion cues from events with the structural details in images, preventing the achievement of optimal low-light image enhancement, as shown in Fig. 1 (c).

To address these limitations, we introduce EvRWKV, a novel framework designed for continuous cross-modal interaction through dual-domain processing. Unlike earlier fusion strategies [16, 42, 33], our EvRWKV achieves noise-robust spatiotemporal alignment through recursive dual-domain interaction and dynamic cross-modal gating, adaptively balancing event motion cues and image textures. It consists of two core modules: the Cross-RWKV module and the Event Image Spectral Fusion Enhancer (EISFE) module. The Cross-RWKV module is at the heart of our approach and pioneers the use of the Receptance Weighted Key Value (RWKV) architecture [37] for cross-modal fusion in low-light enhancement. This module is designed to effectively capture temporal dependencies and enable fine-grained interaction between event and image features. Complementing this, EISFE addresses noise and structural degradation through coordinated frequency-spatial domain processing. In the frequency domain, EISFE employs an Adaptive Gaussian Filter to dynamically suppress noise while preserving structural information. Simultaneously, in the spatial domain, deformable convolutions with learnable offset fields actively align and fuse high-frequency details from both modalities, resolving spatial misalignment. By combining these two core modules, EvRWKV effectively enhances low-light images while addressing noise, structural degradation.

In summary, EvRWKV represents a significant advancement in low-light image enhancement by effectively harnessing the synergistic potential of event and image cameras through a unified, cross-modal, and cross-domain architecture. The contributions of this work are as follows:

- We propose EvRWKV, a novel framework that establishes continuous cross-modal interaction through dual-domain processing for low-light enhancement, establishing intrinsic information exchange between event and image modalities.
- We present Cross-RWKV, an RWKV-based backbone that captures temporal dynamics and performs cross-modal

fusion through simultaneous event-image processing for enhanced low-light performance.

- We develop EISFE, a module operating in frequency and spatial domains to achieve noise mitigation, structure enhancement, and multi-modal feature alignment.
- We demonstrate that EvRWKV achieves state-of-the-art (SOTA) performance on low-light enhancement across real-world datasets (SDE, SDS, RELED), effectively suppressing noise and improving visual quality.

The rest of this paper is organized as follows: Section II details the related work in low image enhancement. Section III describes the workflow for each step of our EvRWKV method. Section IV gives a detailed overview of the experimental results and analysis. In the last section V, we summarize and look forward to our work.

II. RELATED WORK

A. Frame-based Low-light Enhancement

Low-light enhancement (LLE) aims to improve the visibility and quality of images captured in dimly lit environments. Traditional frame-based low-light enhancement methods primarily operate on standard image frames. These methods can be broadly categorized into histogram equalization [2, 1, 4], Gamma Correction [15, 38] and Retinex-based algorithms [11, 50, 8, 54, 31]. The first two methods directly enhance the intensity and contrast of low light image, while the Retinex-based algorithm models the image as a combination of illumination and reflectivity. Although effective in improving visibility, these approaches often encounter limitations in handling complex lighting conditions, especially in scenes with varying illumination or dark regions. Moreover, these methods may amplify noise, particularly in low-light regions, leading to undesirable artifacts.

Recent advancements have been propelled by deep learning, particularly with convolutional neural networks (CNNs) [8, 26, 5] and Transformer architectures [51, 3], which have led to the development of more sophisticated frame-based low-light enhancement methods. Chen et al. [5] established a low light image dataset and proposed a full convolution network for enhancement. Wang et al. [44] proposed to enhance underexposed photos by learning the illumination map. Wang et al. [43] collect SDS dataset by using mechatronic system and proposed a framework integrating progressive alignment and Retinex-based illumination prediction. Cai et al. [3] propose a one-stage Transformer framework Retinexformer for low-light image enhancement, leveraging Retinex theory and illumination-guided attention to suppress noise. However, these frame-only methods fundamentally suffer from information loss in dark regions due to sensor noise floor limitations, leading to irreversible texture degradation and motion blur amplification.

B. Event-guided Low-light Enhancement

The emergence of event cameras has significantly revolutionized low-light perception by offering a new paradigm in image sensing. Unlike traditional frame-based cameras that

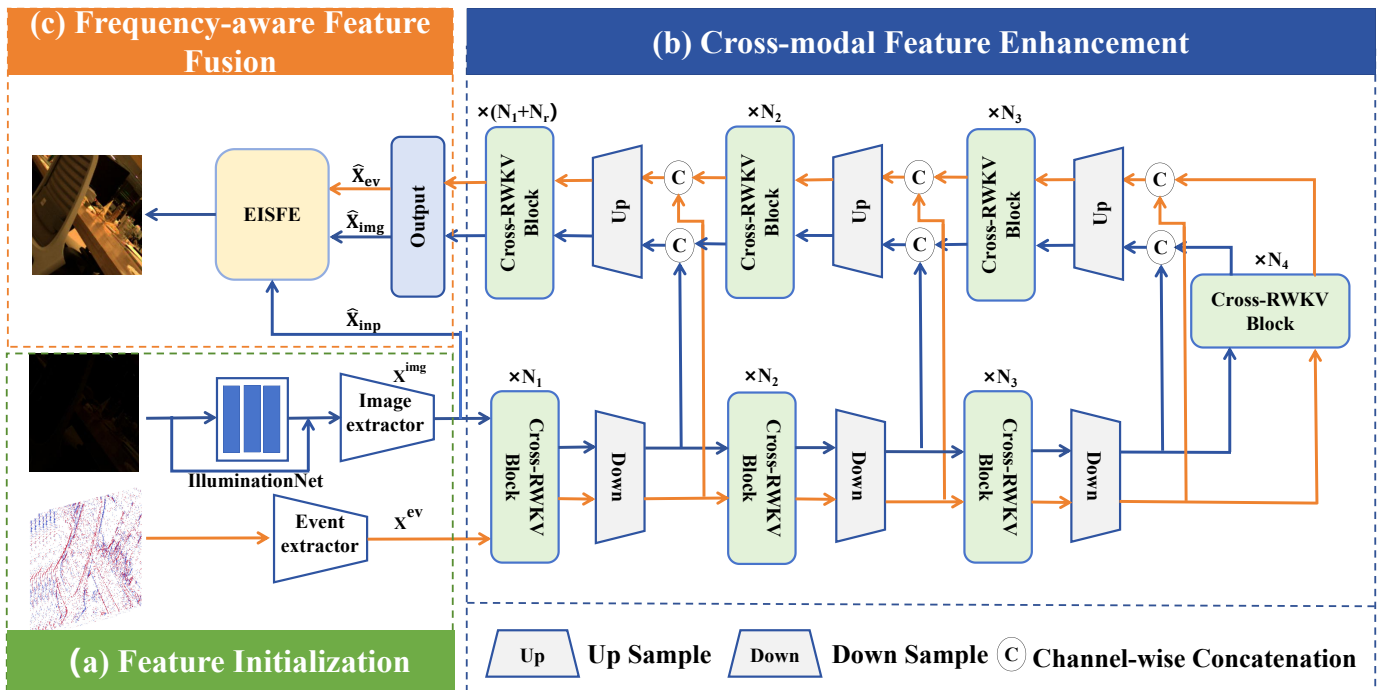


Fig. 2. An overview of our framework. Our method consists of three parts: (a) Feature Initialization (Sec III-A), (b) Cross-modal Feature Restoration (Sec III-B), and (c) Frequency-aware Feature Fusion (Sec III-C). Specifically, Cross-modal Feature Restoration contains multiple Cross-RWKV blocks for feature alignment, and Frequency-aware Feature Fusion integrates image and event features for final output.

capture images at fixed intervals, event cameras detect changes in the scene asynchronously, producing a continuous stream of events that encode pixel-level intensity changes with high temporal resolution. Rebecq et al. [39] propose a recurrent network to reconstruct high speed and high dynamic range videos from event camera data. Event-based approaches for LLE like NER-Net [32] leveraged event streams' temporal continuity to address non-uniform illumination via learnable timestamp calibration. Subsequent works explored hybrid event-frame fusion strategies. Jiang et al. [16] established joint feature learning through attention, while [28] introduced the SDE dataset with precise spatial-temporal alignment and proposed SNR-guided feature selection in EvLight framework. Kim et al. [19] propose an event-guided end-to-end framework for joint low-light video enhancement and deblurring on the real-world RELED dataset, utilizing temporal alignment and cross-modal spectral filtering. However, current fusion architectures are still limited by methods that rely on basic fusion strategies, which fail to effectively separate modality-specific noise patterns. Additionally, many of these approaches suffer from inflexible fusion operators that lack adaptive cross-modal interaction mechanisms. Furthermore, they often underutilize the event streams' intrinsic motion information, hindering comprehensive dynamic scene modeling.

C. Receptance Weighted Key Value

The Receptance Weighted Key Value (RWKV) architecture [37] emerges as a transformative sequential modeling paradigm, synergizing the parallel computation advantages of transformers with the memory efficiency of recurrent networks. Departing from conventional attention mechanisms

constrained by quadratic complexity, RWKV introduces time-shifted receptance gates and exponentially decaying key projections to maintain hidden states [36], enabling linear computational scaling with sequence length. In computer vision, RWKV has demonstrated remarkable versatility across diverse tasks [27]. For instance, Restore-RWKV [53] employs an omnidirectional token translation layer and recurrent WKV attention to restore medical images [52] by capturing spatial dependencies, while PointRWKV [12] leverages linear complexity and multi-head matrix states to enhance geometric feature extraction in 3D point cloud processing. Vision-RWKV [7] further extends its capabilities to high-resolution image analysis by reducing spatial aggregation complexity, outperforming traditional Vision Transformers (ViTs). In real-time video analytics, the TLS-RWKV framework [56] achieves efficient temporal pattern recognition for action detection. StyleRWKV [6] utilizes RWKV models for efficient style transfer, enhancing global and local context while maintaining low memory usage and linear time complexity.

Despite these advances, RWKV's application to cross-modal fusion scenarios—particularly for processing asynchronous, heterogeneous data streams like images and events—remains underdeveloped. Existing RWKV variants struggle with asynchronous temporal alignment and spatial-temporal sparsity gaps. While recent works like RWKV-CLIP [10] explore vision-language alignment, they primarily focus on static multimodal interactions. Our work proposes a novel perspective: establishing continuous event-image synergy, where events resolve temporal ambiguities in blurry regions through high-frequency temporal updates, while images anchor sparse event data to structural priors via spatial-semantic grounding. This

approach aligns with RWKV’s inherent strength in modeling long-range dependencies while mitigating its limitations in handling asynchronous modalities, opening new pathways for applications in motion deblurring, low-light enhancement, and neuromorphic vision systems.

III. METHODOLOGY

We propose *EvRWKV*, a novel framework designed for continuous cross-modal interaction through dual-domain processin that leverages the complementary advantages of low-light images and event streams to achieve robust illumination enhancement and noise suppression. As illustrated in Fig. 2, our framework comprises three key parts: 1) Feature Initialization, 2) Cross-modal Feature Restoration, 3) Frequency-aware Feature Fusion. The framework takes a low-light image I and paired event stream $\{e_k\}_{k=1}^N$ as inputs, producing an enhanced image I_{en} . At first, a series of convolution layers extract features from low light images and event data, and then process them through the 4-level U-shaped encoder-decoder architecture composed of cross-RWKV composed of spatial and channel hybrid components. The output of the architecture passes the EISFE module is enhanced in frequency domain and spatial domain fusion processing to improve image quality.

A. Feature Initialization

Recent low-light enhancement methods demonstrate that preliminary enhancement facilitates subsequent restoration. Following Retinex theory [23], an image $I \in \mathbb{R}^{H \times W \times 3}$ can be decomposed into reflectance $R \in \mathbb{R}^{H \times W \times 3}$ and illumination $L \in \mathbb{R}^{H \times W}$ as $I = R \odot L$, where \odot denotes element-wise multiplication. Following [28], we enhance the low-light image I through:

$$I_{lu} = I \odot \hat{L} + I, \quad (1)$$

where \hat{L} is the estimated illumination map, implementing rough enhancement while preserving original details. The event stream $\{e_k\}$ is converted into a voxel grid $E \in \mathbb{R}^{H \times W \times B}$ ($B = 32$) to preserve spatio-temporal information. The image I_{lu} and event voxel E are both downsampled to $\frac{H}{2} \times \frac{W}{2}$ via a two-layer 3×3 conv with strides 1 & 2, extracting features $X^{img}, X^{ev} \in \mathbb{R}^{\frac{H}{2} \times \frac{W}{2} \times C}$.

B. Cross-modal Feature Restoration

Existing methods for event-image fusion in low-light scenarios often fail to balance computational efficiency and robust cross-modal interaction, particularly in capturing high-frequency motion cues from events and preserving spatial details from images [16, 28]. Furthermore, they frequently treat event and image data as independent streams, failing to fully exploit the fine-grained spatiotemporal relationships between them. To address this, we propose the Cross-RWKV Module, which integrates Re-WKV Attention for capturing global interactions and Cross-Modal Switch Omni-Shift (CS-Shift) for local feature enhancement and multi-modal information interaction. Specifically, multiple Cross-RWKV Modules form a 4-level encoder-decoder. The encoder progressively

downsamples spatial dimensions and expands channels, while the decoder upsamples to restore resolution, enabling multi-scale cross-modal fusion. The outputs $O_{img}, O_{ev} \in \mathbb{R}^{\frac{H}{2} \times \frac{W}{2} \times 2C}$ is split by a 3×3 convolution into $\hat{X}_{img}, \hat{X}_{ev} \in \mathbb{R}^{\frac{H}{2} \times \frac{W}{2} \times C}$. As shown in Fig.3, the module operates through spatial and channel mix, enabling efficient cross-modal fusion of event and image features. The details of the Cross-RWKV Block are as follows:

1) *Spatial Mix*: The overall structure of Spatial Mix is illustrated in the Fig.3. This module aims to establish long-range dependencies across spatial dimensions while enabling effective interaction and information fusion between image and event modalities. Given the input feature sequences $X^{img}, X^{ev} \in \mathbb{R}^{T \times C}$, where $T = \frac{H}{2} \times \frac{W}{2}$ represents the spatial resolution of tokens, the module processes image tokens and event tokens in parallel, first performing spatial-level feature fusion through Layer Normalization (LN) and the CS-shift mechanism.

$$X_s^{img}, X_s^{ev} = \text{CS-Shift}(\text{LN}_1(X^{img}), \text{LN}_2(X^{ev})), \quad (2)$$

where CS-shift is formulated as:

$$\text{CS-Shift}(X_s^{img}, X_s^{ev}) = W^T X^*$$

$$W = \begin{pmatrix} w_1^{img} & w_1^{ev} \\ w_2^{img} & w_2^{ev} \\ w_3^{img} & w_3^{ev} \\ w_4^{img} & w_4^{ev} \end{pmatrix}, \quad X^* = \begin{pmatrix} X_s^{img} & X_s^{ev} \\ \text{Conv}_{1 \times 1}(X_s^{img}) & \text{Conv}_{1 \times 1}(X_s^{ev}) \\ \text{Conv}_{3 \times 3}(X_s^{img}) & \text{Conv}_{3 \times 3}(X_s^{ev}) \\ \text{Conv}_{5 \times 5}(X_s^{img}) & \text{Conv}_{5 \times 5}(X_s^{ev}) \end{pmatrix}, \quad (3)$$

where w_i^{img} and w_i^{ev} represent learnable parameters for scaling specific branches, and $\text{Conv}_{k \times k}()$ denotes depthwise convolution with kernel size k . This CS-shift mechanism captures both local and global features by fusing information under different receptive fields, resulting in accurate token shift outcomes.

Following the shift operation, instead of using standard linear projections, we adopt a depthwise separable convolution to compute keys:

$$K_s^{img} = \text{DPConv}(X_s^{img}), K_s^{ev} = \text{DPConv}(X_s^{ev}), \quad (4)$$

where $\text{DPConv}()$ consists of Depthwise Convolution and Pointwise Convolution, designed to preserve fine-grained spatial structures while efficiently expanding the receptive field.

Meanwhile, the value and receptance vectors for each modality are generated through linear projections:

$$V_s^{img} = X_s^{img} W_v^{img}, \quad R_s^{img} = X_s^{img} W_r^{img}, \quad (5)$$

$$V_s^{ev} = X_s^{ev} W_v^{ev}, \quad R_s^{ev} = X_s^{ev} W_r^{ev}, \quad (6)$$

where $W_{img}^v, W_{img}^r, W_{ev}^v$, and W_{ev}^r are four fully connected layers.

Following the Restore-RWKV [53], we employ the Re-WKV mechanism to compute the global attention result $wkv \in \mathbb{R}^{T \times C}$. At the same time, key representations are directly exchanged between image tokens and event tokens, allowing each modality to attend to the spatial structure of the other modality, thereby enabling joint spatial reasoning between images and events:

$$\text{wkv}^{\text{img}} = \text{Re-WKV}(K_s^{\text{ev}}, V_s^{\text{img}}), \quad (7)$$

$$\text{wkv}^{\text{ev}} = \text{Re-WKV}(K_s^{\text{img}}, V_s^{\text{ev}}) \quad (8)$$

where Re-WKV is implemented by applying the Bi-WKV attention mechanism recurrently along both horizontal and vertical directions. Specifically, the attention output for the t -th token is computed as:

$$\text{wkv}_t = \frac{\sum_{i=1, i \neq t}^T e^{-(|t-i|-1)/T \cdot (w+k_i)} v_i + e^{u+k_t} v_t}{\sum_{i=1, i \neq t}^T e^{-(|t-i|-1)/T \cdot (w+k_i)} + e^{u+k_t}} \quad (9)$$

Here, T denotes the total number of tokens, k_i and v_i are the key and value vectors at position i , and $w \in \mathbb{R}^C$, $u \in \mathbb{R}^C$ are learnable parameters that control the relative positional bias and provide additional weight to the current token, respectively. By applying Bi-WKV iteratively across multiple directions, Re-WKV effectively models long-range dependencies in 2D spatial structures, enabling enhanced global contextual reasoning across modalities.

To further promote cross-modal feature alignment, we introduce learnable fusion gates $\alpha_{\text{img}}, \alpha_{\text{evt}} \in \mathbb{R}^C$, applied to modulate the contribution from each modality during the final representation fusion:

$$X_1 = \sigma(\alpha_{\text{img}}) \cdot \text{wkv}^{\text{img}} + (1 - \sigma(\alpha_{\text{img}})) \cdot X^{\text{ev}}, \quad (10)$$

$$X_2 = \sigma(\alpha_{\text{evt}}) \cdot \text{wkv}^{\text{ev}} + (1 - \sigma(\alpha_{\text{evt}})) \cdot X^{\text{img}} \quad (11)$$

These fused representations are then gated by the learned receptance signals to produce the final outputs:

$$O_{\text{img}} = (\sigma(R_{\text{img}}) \odot X_1) W_o^{\text{img}}, \quad (12)$$

$$O_{\text{evt}} = (\sigma(R_{\text{evt}}) \odot X_2) W_o^{\text{evt}} \quad (13)$$

Where W_o^{img} and W_o^{evt} are linear output projection matrices.

This design enables explicit cross-modal interaction through key exchange, spatially-aware recurrent updates via Re-WKV, and adaptive fusion through gating, yielding a robust mechanism for unified spatial modeling over both image and event streams.

2) *Channel Mix*: The Channel Mix module is designed to model cross-channel interactions within each spatial token while preserving the spatial structure of visual inputs. Unlike the Spatial Mix module that jointly processes both image and event modalities, Channel Mix focuses solely on the image stream. This design choice stems from the observation that channel-wise semantic structures are generally more informative and stable in image data than in sparse and noisy event representations.

Given the image features $X_{\text{img}} \in \mathbb{R}^{T \times C}$, where $T = H \times W$ denotes the number of spatial tokens and C is the channel dimension, the input first undergoes an Omni-Shift operation to enhance local contextual information:

$$X_c^{\text{img}} = \text{OmniShift}(\text{Conv}(X_{\text{img}})) \quad (14)$$

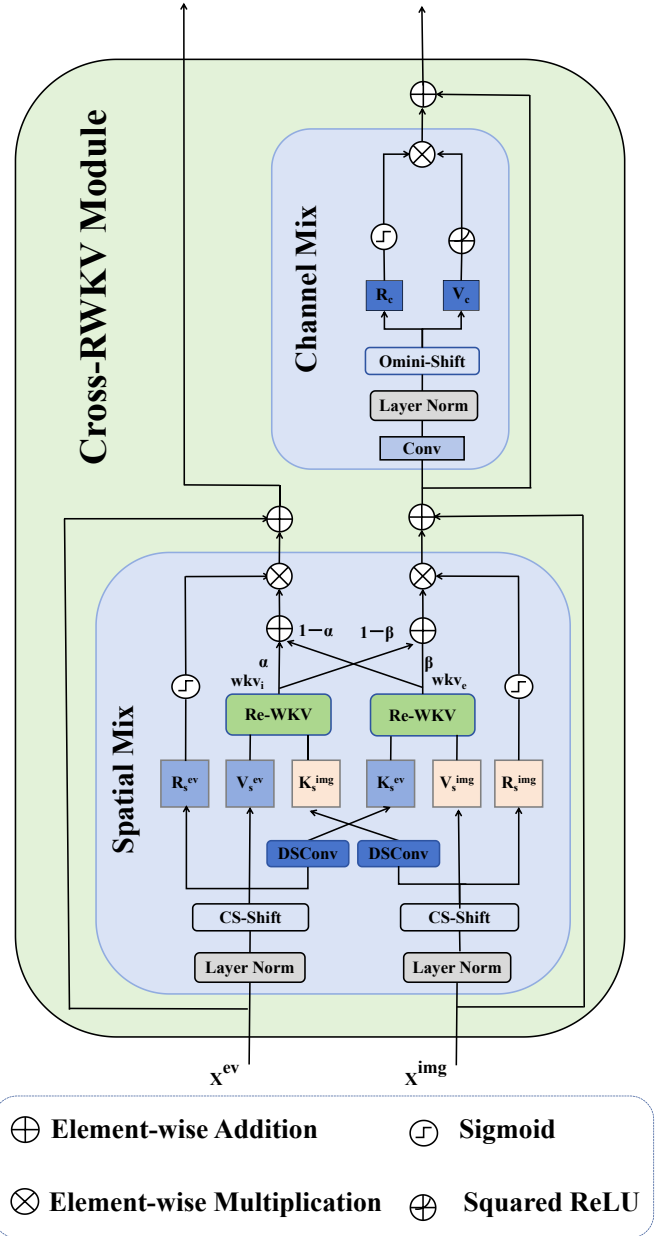


Fig. 3. Architecture of the Cross-RWKV module, which includes Spatial Mix for spatial feature processing and Channel Mix for channel-wise interaction.

The shifted feature is then passed through a gated channel-wise mixing pipeline. A key projection is first applied:

$$K_c = \text{squared ReLU}(X_c^{\text{img}} W_k) \quad (15)$$

where $W_k \in \mathbb{R}^{C \times C_h}$ is the key projection matrix and the squared ReLU non-linearity emphasizes strong activations while suppressing weak ones. This is followed by a value projection to obtain the transformed feature:

$$V_c = K_c W_v, \quad W_v \in \mathbb{R}^{C_h \times C} \quad (16)$$

A separate gating signal is generated through a linear transformation and a sigmoid activation:

$$R_c = \sigma(X_c^{\text{img}} W_r), \quad W_r \in \mathbb{R}^{C \times C} \quad (17)$$

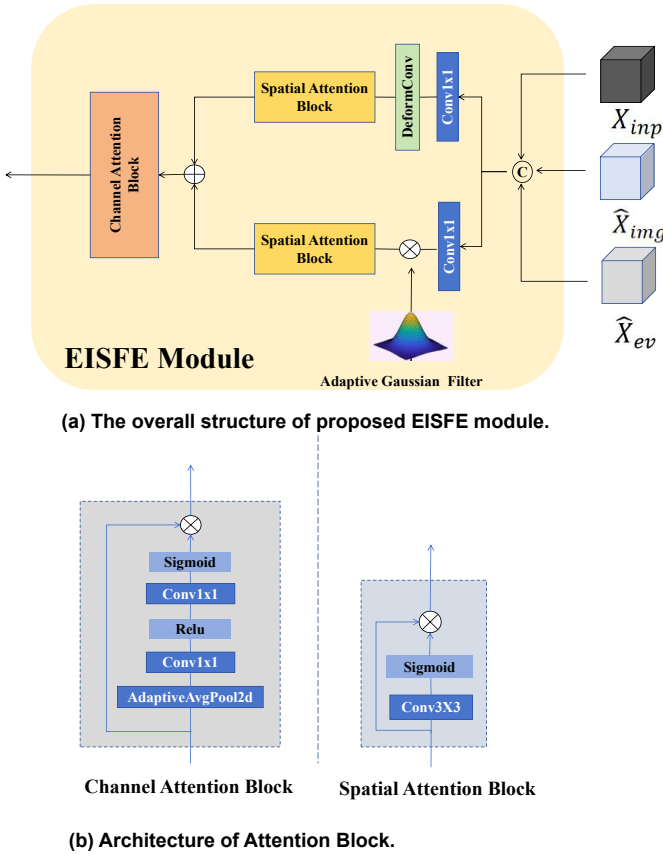


Fig. 4. Overview of the proposed EISFE module. (a) The overall structure includes Channel and Spatial Attention Blocks combined with an Adaptive Gaussian Filter to fuse inputs from image and event features. (b) Details of the Channel Attention Block and Spatial Attention Block architectures.

The final output is obtained via element-wise modulation:

$$O_c = R_c \odot V_c \quad (18)$$

By restricting Channel Mix to the image modality only, we ensure more stable and informative feature transformations. Event streams, while rich in motion cues, often suffer from high sparsity and noise in the channel dimension, making them less suitable for dense feedforward modeling. Therefore, reserving event data for interaction in the spatial domain (via Spatial Mix) while using only image data for channel-wise transformations leads to a better division of modeling responsibilities, improving overall robustness and representation quality.

C. Frequency-aware Feature Fusion

To effectively integrate complementary cues from image and event modalities, we propose the EISFE module, a Frequency-aware Image-Event Spatial-Frequency Enhancement module. This dual-domain fusion mechanism jointly exploits frequency-domain smoothness and spatial-domain adaptivity to enhance reconstruction quality, particularly in challenging scenarios such as motion blur, fast motion, or low-light degradation.

Given the restored image feature \hat{X}_{img} , event feature \hat{X}_{ev} , and raw image input X_{inp} , we first concatenate them along the channel dimension to form a unified representation:

$$X_{fused} = \text{Concat}(\hat{X}_{img}, \hat{X}_{ev}, X_{inp}) \in \mathbb{R}^{3C \times H \times W}.$$

We then apply two separate 1×1 convolutions to decompose X_{fused} into two parallel branches: a frequency branch X_{freq} and a spatial branch X_{spat} .

In the frequency branch, we introduce a channel-wise Adaptive Gaussian Filtering mechanism to selectively suppress noise while preserving structural information. Unlike traditional fixed-filter approaches, our method learns a distinct Gaussian standard deviation σ_c for each channel, enabling content-adaptive filtering across different frequency sensitivities. Given the frequency-branch input $X_{freq} \in \mathbb{R}^{C \times H \times W}$, we generate a 2D Gaussian kernel $G_{\sigma_c} \in \mathbb{R}^{K \times K}$ for each channel using its learned $\sigma_c \in [\sigma_{min}, \sigma_{max}]$, and define it as:

$$G_{\sigma_c}(x, y) = \frac{1}{2\pi\sigma_c^2} \exp\left(-\frac{x^2 + y^2}{2\sigma_c^2}\right),$$

where (x, y) are spatial coordinates.

To efficiently apply filtering, we perform the convolution in the frequency domain via Fast Fourier Transform (FFT). Specifically, for each channel c , the filtered output is computed as:

$$\hat{X}_{freq,c} = \mathcal{F}^{-1}(\mathcal{F}(X_{freq,c}) \cdot \mathcal{F}(G_{\sigma_c})),$$

where $\mathcal{F}(\cdot)$ and $\mathcal{F}^{-1}(\cdot)$ denote 2D FFT and inverse FFT, respectively. This formulation allows the model to perform global frequency-aware filtering with high efficiency and adaptivity.

By learning σ_c per channel, this module dynamically adjusts filtering strength: it smooths flat areas while preserving edge structures and fine details, making it well-suited for denoising and contrast enhancement in degraded conditions.

In parallel, the spatial branch processes X_{spat} using a deformable convolution. This allows flexible receptive fields that adapt to local content, enabling the model to capture fine-grained spatial variations such as motion boundaries or geometric distortions. The output is denoted as:

$$\hat{X}_{spat} = \text{DeformConv}(X_{spat}),$$

which retains high-frequency spatial patterns that complement the globally smoothed features from the frequency branch.

To integrate the outputs of the frequency and spatial branches, we design a hierarchical attention fusion strategy that sequentially applies spatial and channel attention mechanisms. This allows the model to selectively emphasize salient patterns while suppressing irrelevant noise, thereby enhancing cross-modal feature integration. As illustrated in Fig. 4, the fusion begins by computing spatial attention maps independently for both branches:

$$X_{attn-spat} = A_{freq} \odot \hat{X}_{freq} + A_{spat} \odot \hat{X}_{spat}, \quad (19)$$

where $A_{\text{freq}}, A_{\text{spat}}$ denotes spatial attention maps independently for both branches, and \odot represents element-wise multiplication. This formulation adaptively combines spatial details and frequency-aware structures based on per-pixel relevance.

Following the spatial attention stage, we further refine the fused features through channel-wise attention to emphasize globally informative dimensions. As shown in Fig. 4, we first aggregate global context via adaptive global average pooling:

$$X_{\text{attn}} = X_{\text{attn-spat}} \odot A_{\text{chan}}. \quad (20)$$

This two-stage attention mechanism allows the EISFE module to dynamically adapt to both local and global feature importance. The spatial attention modulates each spatial location based on semantic content, while the channel attention globally reweighs feature maps to highlight informative channels. Together, these mechanisms enable robust and adaptive fusion of image-event representations under various degradation conditions.

Finally, the fused feature map $X_{\text{attn}} \in \mathbb{R}^{C \times \frac{H}{2} \times \frac{W}{2}}$ is first linearly projected with a 1×1 convolution to refine channel interactions, then up-sampled to the original spatial resolution by a learnable 4×4 transposed convolution, and finally remapped to the RGB space through another 1×1 convolution.

D. Loss Function

We optimise *EvRWKV* in an end-to-end fashion by minimising a weighted combination of four complementary losses: the pixel-wise reconstruction loss \mathcal{L}_r , the perceptual loss \mathcal{L}_p , the Structural Similarity loss \mathcal{L}_s , and its multi-scale extension \mathcal{L}_m . Specifically,

$$\mathcal{L}_{\text{total}} = \lambda_r \mathcal{L}_r + \lambda_p \mathcal{L}_p + \lambda_s \mathcal{L}_s + \lambda_m \mathcal{L}_m, \quad (21)$$

where the hyper-parameters $\lambda_r, \lambda_p, \lambda_s, \lambda_m$ balance the contributions of the individual terms.

To retain low-level fidelity, we adopt the L1-Charbonnier loss to penalise pixel errors between the enhanced image I_{en} and the ground-truth image I_{gt} :

$$\mathcal{L}_r = \sqrt{\|I_{\text{en}} - I_{\text{gt}}\|^2 + \varepsilon^2}, \quad (22)$$

where $I_{\text{en}}, I_{\text{gt}}$ denote the enhanced and ground truth images and $\varepsilon = 10^{-4}$ ensures numerical stability.

We employ the perceptual loss [24] to preserve the high-level similarity between the fused image and source images, which is given by

$$\mathcal{L}_p = \|\Phi(I_{\text{en}}) - \Phi(I_{\text{gt}})\|_1, \quad (23)$$

where Φ represents feature extraction using the Alex network [21].

For every 11×11 Gaussian window Ω we compute the Structural Similarity (SSIM) index between the enhanced patch $x = I_{\text{en}}|_{\Omega}$ and the corresponding ground-truth patch $y = I_{\text{gt}}|_{\Omega}$:

$$\text{SSIM}(x, y) = \frac{(2\mu_x\mu_y + C_1)(2\sigma_{xy} + C_2)}{(\mu_x^2 + \mu_y^2 + C_1)(\sigma_x^2 + \sigma_y^2 + C_2)}, \quad (24)$$

where μ, σ , and σ_{xy} denote local means, standard deviations and cross-variance, while C_1 and C_2 avoid division by zero.

Averaging the index over all windows and turning it into a loss gives

$$\mathcal{L}_s = 1 - \text{SSIM}(I_{\text{en}}, I_{\text{gt}}). \quad (25)$$

To capture structures at multiple resolutions, we build a five-level Gaussian pyramid and evaluate SSIM at every scale j . The resulting multi-scale similarity is the weighted geometric mean

$$\text{MS-SSIM}(x, y) = \prod_{j=1}^5 \text{SSIM}_j(x, y)^{\omega_j}, \quad (26)$$

where $\{\omega_j\}$ are the standard MS-SSIM weights ($\sum_j \omega_j = 1$). The corresponding loss is obtained by

$$\mathcal{L}_m = 1 - \text{MS-SSIM}(I_{\text{en}}, I_{\text{gt}}). \quad (27)$$

IV. EXPERIMENTS

A. Experimental Settings

1) *Datasets and Evaluation Metrics*: SED [28], SDSD [43], and RELED [19] datasets are selected to test the enhancement performance of our *EvRWKV* framework.

SED dataset contains 91 image-event paired sequences (43 indoor and 48 outdoor) captured with a DAVIS346 event camera at a resolution of 346×260 ; it is primarily used to evaluate the capability of different methods to leverage event cues for low-light enhancement under diverse illumination conditions.

SDSD dataset provides 150 low-light/normal-light paired video sequences with an original resolution of 1920×1080 ; following the dynamic-subset split (125 sequences for training and 25 for testing), all videos are down-sampled to 346×260 , and their event streams are synthesized with the v2e [14] simulator. This dataset evaluates the robustness of enhancement methods in dynamic low-light scenes.

RELED dataset comprises 42 scenes (29 for training and 13 for testing), each offering a low-light blurred input directly paired with a sharp, normal-light reference, making it suitable for benchmarking algorithms that jointly address illumination enhancement and deblurring.

Together, these three benchmarks provide a comprehensive testbed for assessing the multi-modal low-light enhancement capability of our *EvRWKV* method. We use the peak-signal-to-noise ratio (PSNR) [13] and SSIM [48] for evaluation.

2) *Implementation Details*: All experiments were conducted with the Adam optimizer [20]. Learning rates were set to $1e-4$ for SDE datasets, $1.5e-4$ for SDSD datasets, and $1e-4$ for RELED datasets. The framework was trained on an NVIDIA RTX 3090 GPU for 80 training cycles with a batch size of eight. For the training set, we employed data-augmentation techniques consisting of random 256×256 crops, horizontal flips, and rotations of $90^\circ, 180^\circ$, and 270° . For the test set, we applied only a center crop of 256×256 .

3) *State-of-the-Art Methods for Comparisons*: We compared our *EvRWKV* with ten methods, including five methods that only use RGB images as input (SNR-Net [51], Uformer [47], LLLFlow-L-SKF [49], RetinexMac [30], Retinexformer [3]), five methods that use a RGB image and paired events as inputs (ELIE [16], eSL-Net [42], LLVE-SEG [33], ELEDNet

TABLE I
QUANTITATIVE COMPARISON OF DIFFERENT METHODS ON TWO REAL CAPTURED EVENT DATASETS, SDE DATASET AND RELED DATASET. THE BEST AND SECOND BEST RESULTS ARE HIGHLIGHTED IN BOLD AND UNDERLINED RESPECTIVELY.

Method	Publication	Backbone	Inputs		SDE-in		SDE-out		RELED	
			Image	Event	PSNR \uparrow	SSIM \uparrow	PSNR \uparrow	SSIM \uparrow	PSNR \uparrow	SSIM \uparrow
SNR-Net[51]	CVPR2022	Transformer	✓	×	20.05	0.630	22.18	0.661	26.47	0.851
Uformer[47]	CVPR2022	Transformer	✓	×	21.09	0.752	22.32	0.725	28.86	0.832
LLFlow-L-SKF[49]	CVPR2023	CNN	✓	×	20.92	0.661	21.68	0.647	28.62	0.862
Retinexformer[3]	ICCV2023	Transformer	✓	×	21.3	0.692	<u>22.92</u>	0.683	26.66	0.865
RetinexMac[30]	TCSVT2025	Transformer	✓	×	20.61	0.650	21.68	0.683	28.55	0.852
eSL-Net[42]	ECCV2020	CNN	✓	✓	21.42	0.725	21.39	0.681	25.76	0.796
ELIE[16]	TMM2023	Transformer	✓	✓	19.98	0.617	20.69	0.653	26.62	0.862
LLVE-SEG[33]	AAAI2023	Transformer	✓	✓	21.79	0.705	22.35	0.690	29.19	0.875
ELEDNet[19]	ECCV2024	Transformer	✓	✓	21.46	0.7126	22.91	<u>0.726</u>	<u>31.96</u>	<u>0.910</u>
EvLight[28]	CVPR2024	Transformer	✓	✓	<u>22.21</u>	<u>0.758</u>	22.13	0.725	31.29	0.865
Ours	-	RWKV	✓	✓	23.09	0.766	23.43	0.767	32.18	0.910

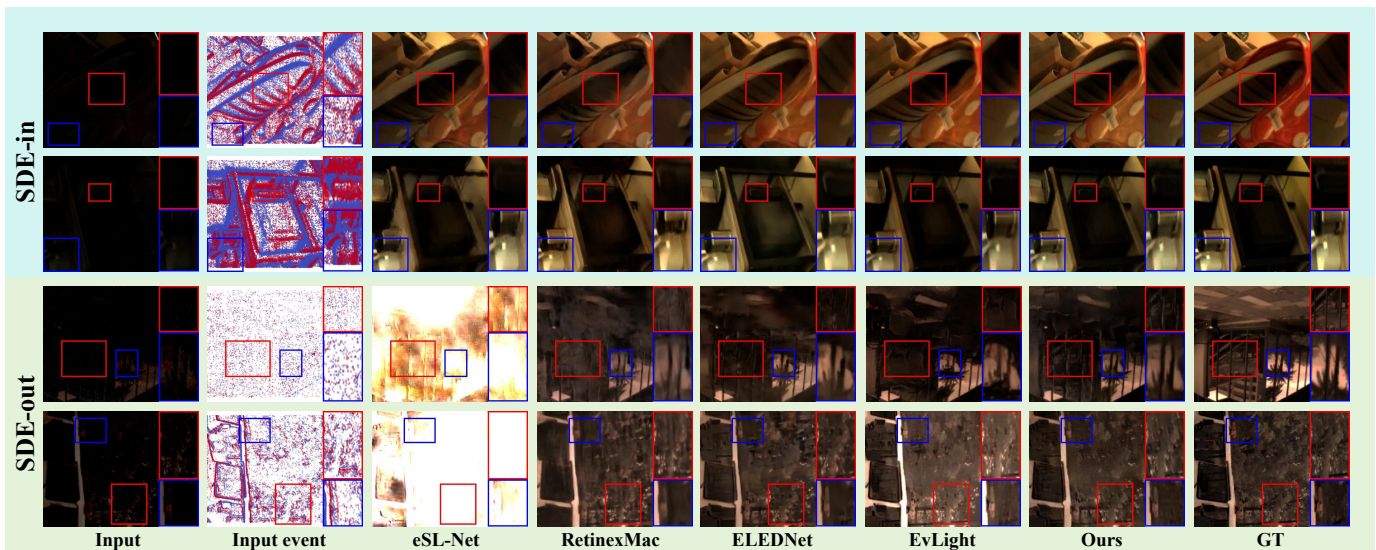


Fig. 5. Visual comparisons with state-of-the-art methods on the SDE dataset.

[19], EvLight [28]). Since the source code of LLVE-SEG [33] is not publicly available, we implemented it according to the description in its paper. For the SNR-Net [51], Uformer [47], LLFlow-L-SKF [49], RetinexMac [30], Retinexformer [3], ELIE [16], eSL-Net [42], ELEDNet [19] and EvLight [28] methods, we used the codes released by the authors to output their results.

B. Quantitative and Qualitative Evaluation

We evaluate the proposed **EvRWKV** framework on three challenging datasets—SDE, SDS, and RELED—covering diverse low-light enhancement scenarios. SDE and RELED contain real-world event-image pairs captured under indoor/outdoor and low-light blurry conditions respectively, while SDS consists of synthetic events generated from

dynamic video sequences. We use PSNR and SSIM as quantitative metrics and provide detailed qualitative analysis to validate the effectiveness of our approach.

1) *Evaluation on the SDE Dataset:* For low-light image enhancement on the SDE dataset, the ability to simultaneously suppress noise and preserve fine structural details is the key evaluation criterion. We first qualitatively compare our EvRWKV method with several representative approaches including eSL-Net [42], ELEDNet [19], EvLight [28], and RetinexMac [30]. As shown in Fig. 5, RetinexMac and ELEDNet reduce noise to some extent but tend to oversmooth textures, resulting in loss of important details in dark regions. As shown in Fig. 5, EvLight maintains more structural information but suffers from residual noise and blur artifacts. eSL-Net, with a relatively small model size, provides limited enhancement capabilities and often underperforms in challenging scenes.

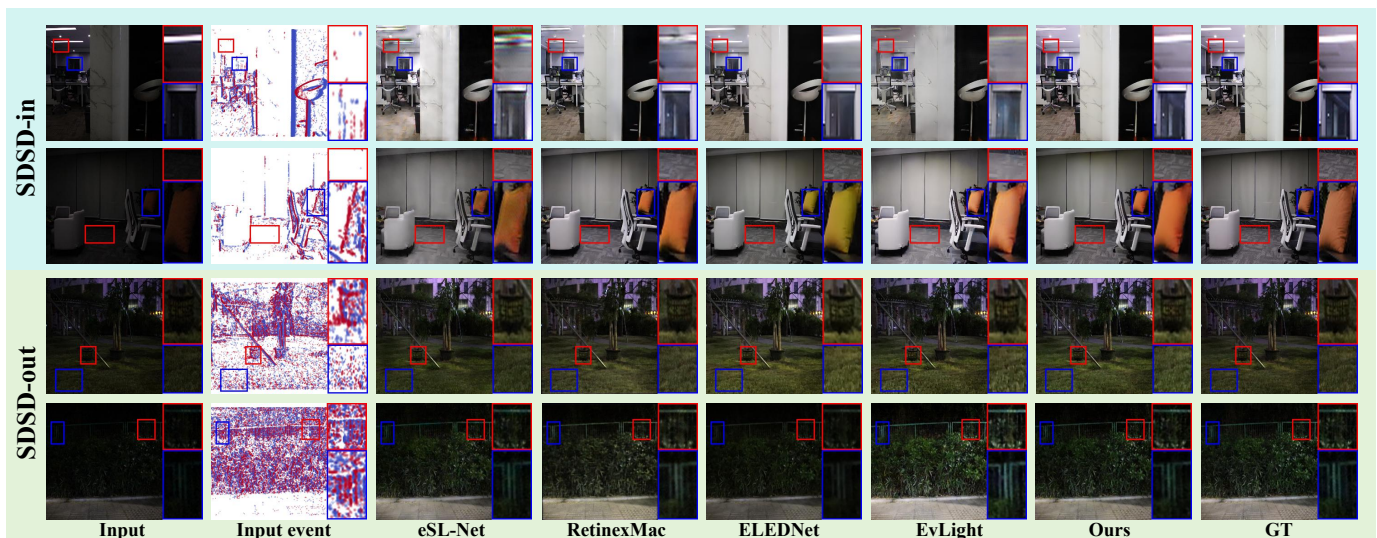


Fig. 6. Visual comparisons with state-of-the-art methods on the SSSD dataset.

TABLE II

QUANTITATIVE COMPARISON OF DIFFERENT METHODS ON THE SSSD DATASET. THE BEST AND SECOND BEST RESULTS ARE HIGHLIGHTED IN BOLD AND UNDERLINED RESPECTIVELY.

Method	Publication	SSSD-in		SSSD-out	
		PSNR \uparrow	SSIM \uparrow	PSNR \uparrow	SSIM \uparrow
SNR-Net[51]	CVPR'22	24.74	0.830	24.82	0.740
Uformer[47]	CVPR'22	24.03	0.900	24.08	0.818
LLFlow-L-SKF[49]	CVPR'23	23.39	0.818	20.39	0.634
Retinexformer[3]	ICCV'23	25.90	0.852	26.08	0.815
RetinexMac[30]	TCSVT'25	27.61	0.900	24.75	0.783
ELIE[16]	TMM'23	27.46	0.879	23.29	0.742
eSL-Net[42]	ECCV'20	23.68	0.821	24.95	0.805
LLVE-SEG[33]	AAAI'23	27.58	0.888	23.51	0.726
ELEDNet[19]	ECCV'24	<u>28.52</u>	<u>0.912</u>	25.08	<u>0.828</u>
EvLight[28]	CVPR'24	28.49	0.909	<u>25.17</u>	0.817
Ours	-	28.96	0.920	27.93	0.839

In contrast, our EvRWKV method achieves a better balance between noise suppression and texture preservation, producing cleaner, brighter images with rich details and minimal artifacts. This demonstrates the effectiveness of our dual-domain fusion and adaptive gating mechanisms in handling complex low-light scenarios.

In terms of quantitative evaluation, Table I lists the PSNR and SSIM scores of different methods on the SDE dataset under both SDE-in and SDE-out settings. Our method achieves the highest scores of 23.09 PSNR and 0.766 SSIM for SDE-in, as well as 23.43 PSNR and 0.767 SSIM for SDE-out. These results outperform all compared methods including SNR-Net [51], Uformer [47], LLFlow-L-SKF [49], LLVE-SEG [33], Retinexformer [3], ELIE [16], LLVE-SEG [33], and the aforementioned qualitative comparison models. The significant improvements in both perceptual quality and objective metrics validate the superiority of our EvRWKV framework in low-light image enhancement.

2) *Evaluation on the SSSD Dataset:* We further qualitatively compare the performance of different methods on the SSSD dataset for low-light image enhancement under challenging lighting and motion conditions. In Fig. 6, we observe that most methods improve the visibility and brightness of degraded images. However, RetinexMac [30], ELEDNet [19], and EvLight [28] exhibit limitations: As shown in Fig. 6, RetinexMac and ELEDNet tend to over-smooth textures and lose fine details, While EvLight, although preserving more structural information, causes noticeable color distortion in some regions. As shown in Fig. 6, eSL-Net [42] shows relatively limited enhancement capability due to its smaller model size. In comparison, our EvRWKV method delivers superior noise suppression and detail preservation, effectively enhancing both static and dynamic scene elements without introducing artifacts. The enhanced images show clearer textures, better contrast, and natural brightness, demonstrating the robustness of our dual-domain cross-modal fusion strategy.

Table II presents the PSNR and SSIM scores of different methods evaluated on the SSSD dataset. Our method achieves the highest scores in both SSSD-in and SSSD-out scenarios, with PSNR values of 28.96 and 27.93, and SSIM values of 0.920 and 0.839, respectively. These results outperform all other compared methods, validating the strong restoration ability and noise robustness of our EvRWKV framework under various low-light conditions. Overall, our approach demonstrates both qualitative and quantitative advantages over existing state-of-the-art techniques on the SSSD dataset.

3) *Evaluation on the RELED Dataset:* To comprehensively evaluate the enhancement performance of our EvRWKV method on the RELED dataset, we compare it qualitatively with several representative approaches including eSL-Net [42], ELEDNet [19], EvLight [28], and RetinexMac [30]. As shown in Fig. 7, the RELED dataset contains extremely low-light images with severe motion blur and noise. As shown in Fig. 7, eSL-Net often causes overexposure while attempting to enhance brightness. RetinexMac boosts overall brightness but



Fig. 7. Visual comparisons with state-of-the-art methods on the Reled dataset.



Fig. 8. Visualization of ablation results.

fails to eliminate noticeable blur. ELEDNet and EvLight aim to balance illumination, but this often leads to the loss of finer details. In contrast, our EvRWKV method effectively leverages event-based motion cues and image textures to suppress noise, reduce blur, and restore fine details, producing visually clearer, sharper, and more natural images without color artifacts or overexposure.

Table I reports the PSNR and SSIM scores for different methods on the RELED dataset. Our EvRWKV achieves the best quantitative results with a PSNR of 32.18 and SSIM of 0.910, significantly outperforming other methods including eSL-Net, ELEDNet, EvLight, and RetinexMac. These quantitative gains demonstrate the robustness and generalization capability of our dual-domain cross-modal fusion framework in handling challenging low-light and motion-degraded scenarios. Overall, our method achieves excellent qualitative and quantitative results across all three real-world low-light enhancement benchmarks.

C. Ablation Study

We conduct comprehensive ablation studies on the SDS-in dataset to evaluate the contribution of each key component in our EvRWKV framework. In particular, we assess the effectiveness of the EISFE module, the SpatialMix and ChannelMix mechanisms within the Cross-RWKV module, and the role of each individual loss term in the overall objective function. For each study, we remove or modify a single module while keeping the rest of the framework unchanged to isolate its impact. The results clearly demonstrate the necessity and complementarity of these components in achieving robust and high-quality low-light enhancement. As shown in Fig. 8, the removal of EISFE (b) results in color distortion. Without SpatialMix (c), visible noise and blurred textures appear, while omitting ChannelMix (d) leads to flat tonal rendering. The full model (e) demonstrates the best visual clarity and color fidelity, especially in complex shadow regions.

1) *Impact of EISFE Module:* To assess the contribution of frequency-aware fusion, we remove the EISFE module and directly decode the features after the Cross-RWKV backbone. As shown in Table III, the absence of EISFE leads to a 1.61 dB drop in PSNR and 0.026 reduction in SSIM. This indicates the importance of frequency-domain filtering and spatial deformable convolution in denoising and structure restoration. Visually, the model without EISFE shows residual noise and blurred edges.

2) *Impact of SpatialMix and ChannelMix:* To verify the effectiveness of the spatial and channel interaction designs in Cross-RWKV, we conduct ablation studies by individually removing each module. As shown in Table III, removing the SpatialMix results in a 2.08 dB PSNR drop and 0.122 SSIM decline, highlighting its critical role in capturing long-range dependencies and facilitating event-image alignment. On the other hand, removing ChannelMix leads to a 2.36 dB decrease in PSNR and a 0.024 SSIM reduction, indicating its importance in refining semantic consistency across feature channels. These results confirm that both modules contribute

TABLE III
ABLATION STUDY OF KEY COMPONENTS ON THE SDS-D-IN DATASET.

Model Variant	PSNR \uparrow	SSIM \uparrow
w/o EISFE	27.35	0.894
w/o SpatialMix	26.88	0.798
w/o ChannelMix	26.60	0.896
Ours	28.96	0.920

TABLE IV
ABLATION STUDY OF LOSS FUNCTIONS ON THE SDS-D-IN DATASET.

Model Variant	PSNR \uparrow	SSIM \uparrow
w/o reconstruction loss (L_r)	26.84	0.896
w/o perceptual loss (L_p)	26.18	0.885
w/o SSIM loss (L_s)	26.06	0.876
w/o MS-SSIM loss (L_m)	27.84	0.899
Ours	28.96	0.920

distinctly and significantly to performance. As illustrated in Fig. 8, ChannelMix aids in preserving local contrast, while SpatialMix enhances spatial structure and reduces texture inconsistency.

3) *Impact of Loss Functions*: To evaluate the contribution of each loss term, we progressively remove pixel, perceptual, SSIM, and MS-SSIM losses from the training objective. The results are summarized in Table IV. Removing the reconstruction loss L_r results in the lowest performance, with a PSNR of 26.84 and an SSIM of 0.896. Excluding the perceptual loss L_p leads to a slight reduction in performance, with a PSNR of 26.18 and an SSIM of 0.885. Removing the SSIM loss L_s results in a PSNR of 26.06 and an SSIM of 0.876, reflecting a loss in structural preservation. Finally, excluding the multi-scale SSIM loss L_m leads to a PSNR of 27.84 and an SSIM of 0.899. The full model, with all losses included, achieves the best results with a PSNR of 28.96 and an SSIM of 0.920, demonstrating a 0.84 dB gain in PSNR over the setting without L_r . This confirms the complementary benefits of each loss term in guiding high-quality reconstruction.

D. Limitations

While EvRWKV performs well across diverse low-light conditions, it encounters challenges in extremely dark scenes with sparse event activity and limited structural cues. In such cases, the framework may struggle to recover fine details or accurate colors, occasionally leading to over-smoothing or artifacts. Additionally, severe motion blur or sensor noise can impair spatial-temporal alignment. Future work will focus on improving robustness through uncertainty modeling and adaptive fusion strategies for broader generalization.

V. CONCLUSION

In this paper, we proposed EvRWKV, a novel and effective framework for low-light image enhancement that leverages continuous cross-modal interaction between event streams

and low-light images through dual-domain processing. Our approach uniquely integrates the RWKV architecture with the EISFE module, enabling adaptive and robust fusion of asynchronous event data and standard images. The Cross-RWKV module effectively captures fine-grained temporal and spatial dependencies, while the EISFE module jointly performs noise suppression and structural restoration via frequency-domain filtering and spatial deformable convolutions. Extensive experiments on multiple challenging real-world low-light datasets demonstrate that EvRWKV significantly outperforms existing state-of-the-art methods in both quantitative metrics and visual quality, effectively suppressing noise, enhancing contrast, and restoring fine details even under severe degradation such as motion blur and extreme darkness. Our dual-domain fusion and adaptive gating mechanisms successfully balance complementary information from event and image modalities, resulting in superior enhancement robustness and generalization. In future work, we plan to explore further improvements in cross-modal fusion strategies and extend the application of the EvRWKV framework to other challenging imaging tasks such as real-time video enhancement and dynamic scene understanding in extreme lighting conditions.

REFERENCES

- [1] Mohammad Abdullah-Al-Wadud et al. “A dynamic histogram equalization for image contrast enhancement”. In: *IEEE transactions on consumer electronics* 53.2 (2007), pp. 593–600.
- [2] Tarik Arici, Salih Dikbas, and Yucel Altunbasak. “A histogram modification framework and its application for image contrast enhancement”. In: *IEEE Transactions on image processing* 18.9 (2009), pp. 1921–1935.
- [3] Yuanhao Cai et al. “Retinexformer: One-stage retinex-based transformer for low-light image enhancement”. In: *Proceedings of the IEEE/CVF international conference on computer vision*. 2023, pp. 12504–12513.
- [4] Turgay Celik and Tardi Tjahjadi. “Contextual and variational contrast enhancement”. In: *IEEE Transactions on Image Processing* 20.12 (2011), pp. 3431–3441.
- [5] Chen Chen et al. “Learning to see in the dark”. In: *Proceedings of the IEEE conference on computer vision and pattern recognition*. 2018, pp. 3291–3300.
- [6] Miaomiao Dai, Qianyu Zhou, and Lizhuang Ma. “StyleRWKV: High-Quality and High-Efficiency Style Transfer with RWKV-like Architecture”. In: *arXiv preprint arXiv:2412.19535* (2024).
- [7] Yuchen Duan et al. “Vision-rwkv: Efficient and scalable visual perception with rwkv-like architectures”. In: *arXiv preprint arXiv:2403.02308* (2024).
- [8] Xueyang Fu et al. “A weighted variational model for simultaneous reflectance and illumination estimation”. In: *Proceedings of the IEEE conference on computer vision and pattern recognition*. 2016, pp. 2782–2790.
- [9] Guillermo Gallego et al. “Event-based vision: A survey”. In: *IEEE transactions on pattern analysis and machine intelligence* 44.1 (2020), pp. 154–180.

- [10] Tiancheng Gu et al. “RWKV-CLIP: a robust vision-language representation learner”. In: *arXiv preprint arXiv:2406.06973* (2024).
- [11] Xiaojie Guo, Yu Li, and Haibin Ling. “LIME: Low-light image enhancement via illumination map estimation”. In: *IEEE Transactions on image processing* 26.2 (2016), pp. 982–993.
- [12] Qingdong He et al. “Pointtrkv: Efficient rwkv-like model for hierarchical point cloud learning”. In: *Proceedings of the AAAI Conference on Artificial Intelligence*. Vol. 39. 3. 2025, pp. 3410–3418.
- [13] Alain Hore and Djemel Ziou. “Image quality metrics: PSNR vs. SSIM”. In: *2010 20th international conference on pattern recognition*. IEEE. 2010, pp. 2366–2369.
- [14] Yuhuang Hu, Shih-Chii Liu, and Tobi Delbruck. “v2e: From video frames to realistic DVS events”. In: *Proceedings of the IEEE/CVF conference on computer vision and pattern recognition*. 2021, pp. 1312–1321.
- [15] Shih-Chia Huang, Fan-Chieh Cheng, and Yi-Sheng Chiu. “Efficient contrast enhancement using adaptive gamma correction with weighting distribution”. In: *IEEE transactions on image processing* 22.3 (2012), pp. 1032–1041.
- [16] Yu Jiang et al. “Event-based low-illumination image enhancement”. In: *IEEE Transactions on Multimedia* 26 (2023), pp. 1920–1931.
- [17] Zhe Jiang et al. “Learning event-based motion deblurring”. In: *Proceedings of the IEEE/CVF Conference on Computer Vision and Pattern Recognition*. 2020, pp. 3320–3329.
- [18] Taewoo Kim et al. “Event-guided deblurring of unknown exposure time videos”. In: *European Conference on Computer Vision*. Springer. 2022, pp. 519–538.
- [19] Taewoo Kim et al. “Towards Real-World Event-Guided Low-Light Video Enhancement and Deblurring”. In: *European Conference on Computer Vision*. Springer. 2024, pp. 433–451.
- [20] Diederik P Kingma. “Adam: A method for stochastic optimization”. In: *arXiv preprint arXiv:1412.6980* (2014).
- [21] Alex Krizhevsky, Ilya Sutskever, and Geoffrey E Hinton. “Imagenet classification with deep convolutional neural networks”. In: *Advances in neural information processing systems* 25 (2012).
- [22] Mohit Lamba and Kaushik Mitra. “Restoring extremely dark images in real time”. In: *Proceedings of the IEEE/CVF conference on computer vision and pattern recognition*. 2021, pp. 3487–3497.
- [23] Edwin H Land and John J McCann. “Lightness and retinex theory”. In: *Journal of the Optical society of America* 61.1 (1971), pp. 1–11.
- [24] Christian Ledig et al. “Photo-realistic single image super-resolution using a generative adversarial network”. In: *Proceedings of the IEEE conference on computer vision and pattern recognition*. 2017, pp. 4681–4690.
- [25] Chongyi Li et al. “Low-light image and video enhancement using deep learning: A survey”. In: *IEEE transactions on pattern analysis and machine intelligence* 44.12 (2021), pp. 9396–9416.
- [26] Mading Li et al. “Structure-revealing low-light image enhancement via robust retinex model”. In: *IEEE transactions on image processing* 27.6 (2018), pp. 2828–2841.
- [27] Zhiyuan Li et al. “A Survey of Rwkv”. In: *arXiv preprint arXiv:2412.14847* (2024).
- [28] Guoqiang Liang et al. “Towards robust event-guided low-light image enhancement: a large-scale real-world event-image dataset and novel approach”. In: *Proceedings of the IEEE/CVF Conference on Computer Vision and Pattern Recognition*. 2024, pp. 23–33.
- [29] Patrick Lichtsteiner, Christoph Posch, and Tobi Delbruck. “A 128x128 120 dB 15us latency asynchronous temporal contrast vision sensor”. In: *IEEE journal of solid-state circuits* 43.2 (2008), pp. 566–576.
- [30] Chunxiao Liu et al. “Efficient Retinex-Based Framework for Low-Light Image Enhancement Without Additional Networks”. In: *IEEE Transactions on Circuits and Systems for Video Technology* 35.5 (2025), pp. 4896–4909. DOI: [10.1109/TCSVT.2024.3520802](https://doi.org/10.1109/TCSVT.2024.3520802).
- [31] Chunxiao Liu et al. “Efficient Retinex-Based Framework for Low-Light Image Enhancement without Additional Networks”. In: *IEEE Transactions on Circuits and Systems for Video Technology* (2024).
- [32] Haoyue Liu et al. “Seeing motion at nighttime with an event camera”. In: *Proceedings of the IEEE/CVF Conference on Computer Vision and Pattern Recognition*. 2024, pp. 25648–25658.
- [33] Lin Liu et al. “Low-light video enhancement with synthetic event guidance”. In: *Proceedings of the AAAI Conference on Artificial Intelligence*. Vol. 37. 2. 2023, pp. 1692–1700.
- [34] Yunfan Lu et al. “Learning spatial-temporal implicit neural representations for event-guided video super-resolution”. In: *Proceedings of the IEEE/CVF Conference on Computer Vision and Pattern Recognition*. 2023, pp. 1557–1567.
- [35] Xinglong Luo et al. “Learning optical flow from event camera with rendered dataset”. In: *Proceedings of the IEEE/CVF International Conference on Computer Vision*. 2023, pp. 9847–9857.
- [36] Bo Peng et al. “Eagle and finch: Rwkv with matrix-valued states and dynamic recurrence”. In: *arXiv preprint arXiv:2404.05892* 3 (2024).
- [37] Bo Peng et al. “Rwkv: Reinventing rnns for the transformer era”. In: *arXiv preprint arXiv:2305.13048* (2023).
- [38] Shanto Rahman et al. “An adaptive gamma correction for image enhancement”. In: *EURASIP Journal on Image and Video Processing* 2016 (2016), pp. 1–13.
- [39] Henri Rebecq et al. “High speed and high dynamic range video with an event camera”. In: *IEEE transactions on pattern analysis and machine intelligence* 43.6 (2019), pp. 1964–1980.

- [40] Cedric Scheerlinck et al. “CED: Color event camera dataset”. In: *Proceedings of the IEEE/CVF Conference on Computer Vision and Pattern Recognition Workshops*. 2019, pp. 0–0.
- [41] Timo Stoffregen et al. “Reducing the sim-to-real gap for event cameras”. In: *Computer Vision—ECCV 2020: 16th European Conference, Glasgow, UK, August 23–28, 2020, Proceedings, Part XXVII 16*. Springer. 2020, pp. 534–549.
- [42] Bishan Wang et al. “Event enhanced high-quality image recovery”. In: *Computer Vision—ECCV 2020: 16th European Conference, Glasgow, UK, August 23–28, 2020, Proceedings, Part XIII 16*. Springer. 2020, pp. 155–171.
- [43] Ruixing Wang et al. “Seeing dynamic scene in the dark: A high-quality video dataset with mechatronic alignment”. In: *Proceedings of the IEEE/CVF international conference on computer vision*. 2021, pp. 9700–9709.
- [44] Ruixing Wang et al. “Underexposed photo enhancement using deep illumination estimation”. In: *Proceedings of the IEEE/CVF conference on computer vision and pattern recognition*. 2019, pp. 6849–6857.
- [45] Tao Wang et al. “Ultra-high-definition low-light image enhancement: A benchmark and transformer-based method”. In: *Proceedings of the AAAI conference on artificial intelligence*. Vol. 37. 3. 2023, pp. 2654–2662.
- [46] Yinglong Wang et al. “Low-light image enhancement with illumination-aware gamma correction and complete image modelling network”. In: *Proceedings of the IEEE/CVF International Conference on Computer Vision*. 2023, pp. 13128–13137.
- [47] Zhendong Wang et al. “Uformer: A general u-shaped transformer for image restoration”. In: *Proceedings of the IEEE/CVF conference on computer vision and pattern recognition*. 2022, pp. 17683–17693.
- [48] Zhou Wang et al. “Image quality assessment: from error visibility to structural similarity”. In: *IEEE transactions on image processing* 13.4 (2004), pp. 600–612.
- [49] Yuhui Wu et al. “Learning semantic-aware knowledge guidance for low-light image enhancement”. In: *Proceedings of the IEEE/CVF Conference on Computer Vision and Pattern Recognition*. 2023, pp. 1662–1671.
- [50] Jun Xu et al. “Star: A structure and texture aware retinex model”. In: *IEEE Transactions on Image Processing* 29 (2020), pp. 5022–5037.
- [51] Xiaogang Xu et al. “Snr-aware low-light image enhancement”. In: *Proceedings of the IEEE/CVF conference on computer vision and pattern recognition*. 2022, pp. 17714–17724.
- [52] Yuezhe Yang et al. “Explicit and Implicit Representations in AI-based 3D Reconstruction for Radiology: A systematic literature review”. In: *arXiv preprint arXiv:2504.11349* (2025).
- [53] Zhiwen Yang et al. “Restore-rwkv: Efficient and effective medical image restoration with rwkv”. In: *arXiv preprint arXiv:2407.11087* (2024).
- [54] Zunjin Zhao et al. “RetinexDIP: A unified deep framework for low-light image enhancement”. In: *IEEE Transactions on Circuits and Systems for Video Technology* 32.3 (2021), pp. 1076–1088.
- [55] Xu Zheng et al. “Deep learning for event-based vision: A comprehensive survey and benchmarks”. In: *arXiv preprint arXiv:2302.08890* (2023).
- [56] Ziqi Zhu, Wuchang Shao, and Dongdong Jiao. “Tls-rwkv: Real-time online action detection with temporal label smoothing”. In: *Neural Processing Letters* 56.2 (2024), p. 57.